Online ISSN 1848-3380, Print ISSN 0005-1144
ATKAFF 57(4), 1007–1019(2016)

Dianwei Qian, Shiwen Tong, Chang Xu

Robust Multi-robot Formations via Sliding Mode Controller and Fuzzy Compensator

DOI 10.7305/automatika.2017.12.1637
UDK [681.516.77.07-55:510.644.4]:621.865.8-182.35-045.7

Original scientific paper

To form up a multiple-robot system, a robust adaptive control scheme is addressed. The control scheme is based on the methodology of sliding mode control (SMC). The formation system is leader-follower-based, whose dynamics are subject to uncertainties. A fuzzy compensator is adopted to approximate the uncertainties. To attenuate the approximation error, a robust adaptive law of the fuzzy compensator is introduced. In the sense of Lyapunov, not only such a control scheme can asymptotically stabilize the whole formation system, but also the convergence of the approximation error can be guaranteed. Compared with the sole sliding mode controller without compensator, some numerical simulations verify the feasibility and effectiveness of the control scheme for the multiple-robot system in the presence of uncertainties.

Key words: Multiple-robot system, Sliding mode, Leader-follower formation, Uncertainties, Fuzzy compensator

Robusno upravljanje višerobotskim formacijama korištenjem klizećeg regulatora i neizrazitog kompenzatora. Kako bi se formirao višerobotski sustav korištena je robusna adaptivna shema upravljanja. Upravljačka shema je bazirana na metodologiji upravljanja klizećim režimom (SMC). Formacijski sustav baziran je na vođa-sljedbenik metodi čija je dinamika podložna nesigurnostima. Za aproksimiranje nesigurnosti korišten je neizraziti kompenzator. Kako bi se prigušila aproksimacijska greška razvijen je robusni adaptivni upravljački zakon. Korištenjem takvog upravljačkog zakona ostvarena je stabilnost prema Lyapunovu, te je moguće garantirati konvergenciju aproksimacijske greške. U usporedbi s regulatorom zasnovanim na klizećem režimu bez kompenzatora, neke numeričke simulacije potvrđuju izvedivost i efikasnost ovakve sheme upravljanja višerobotskim sustavom uz prisutnost nesigurnosti.

Ključne riječi: Višerobotski sustav, Klizeći režim, Vođa-sljedbenik formacija, Nesigurnosti, Neizraziti regulator

1 INTRODUCTION

A multi-robot system composed of several mobile robots can perform collaborative tasks in manufacturing, surveillance and space exploration. Such coordination among the robots is an important and promising research field [1–3]. Compared to a complex single-robot system, the ability of coordinating the robots is superior, including but not limited to economy, effectiveness and efficiency [4, 5]. There are many cooperative tasks like formation, coverage and target aggregation, where the formation control problem stands out because the robots can efficiently accomplish cooperative tasks by forming up and maintaining some formations [6, 7].

Up to now, various formation schemes have been presented and carried out. They can roughly be classified as behavior-based methods, virtual structure techniques and leader-follower schemes [4, 8]. Among them, the leader-follower approaches have become the most popular ones because the idea is simple enough to permit complete analyses and experiments, but the internal formation stability can be theoretically guaranteed [9, 10].

The basic idea of the leader-follower formations [8, 11] is that one robot in a multi-robot system is selected as leader and the other robots are called followers. The leader is responsible for guiding the formation and the followers are required to track the leader in the desired distance l and the desired relative angle ψ. Accordingly, there are two kinds of control frameworks, i.e., $l-l$ and $l-\psi$. Considering the leader-follower approaches, a characteristic is that the formation problem of the multi-robot system is transformed into the independent trajectory tracking problem of each follower robot [4, 8–11]. Although the basic idea is in dispute over its 'single point of failure', such characteristic benefits the formation problem a lot.

Concerning the leader-follower formation maneuvers, various control methods have been reported, i.e., model

predictive control [10], feedback linearization control [12], backstepping control [13], decentralized control [14], intelligent control [15, 16] and sliding mode control (SMC) [17–20], to name but a few. Since SMC is of invariance to matched uncertainties [21, 22], the SMC method has been paid more and more attention. This paper investigates the application of SMC for the leader-follower formation control problem of multiple robots.

Uncertainties are inevitable in practice [23]. The leader-follower formation maneuvers are subject to uncertainties [24]. The uncertainties include parameter fluctuations, model uncertainties and random external disturbances, which turn out to be mismatched [11]. Since the mismatched uncertainties cannot be suppressed by the invariance of SMC, a critical assumption in the aforementioned reports [17–20] is that the uncertainties must have a known boundary in order to guarantee the formation stability. However, the assumption is not mild because the boundary value is hard to exactly know in advance. The lack of the important information may cause several drawbacks such as deficiency of the system stability, decrease of the system robustness and deterioration of the system performance. In order to take SMC into account for the formation control problem, it is necessary to approximate and compensate the uncertainties.

The methodology of fuzzy logic can effectively handle complex nonlinear systems with uncertainties [25, 26]. Some real applications have been reported, such as MEMS triaxial gyroscope system [27], mechanical manipulator [28] and vector voltmeter [29]. In order to attack the uncertainties of the SMC-based formation control problem, this paper considers the fuzzy logic method as an alternative choice. So far, how to overcome the adverse effects triggered by such mismatched uncertainties still remains unsolved and problematic for the SMC-based formation maneuvers.

Since an adaptive fuzzy inference system can approximate a wide class of nonlinear systems via arbitrary closeness [27], this paper proposes a multiple-input multiple-output fuzzy inference system to compensate the uncertainties. The fuzzy system has to adaptively approximate the uncertainties because the assumption that the uncertainties have an unknown boundary holds true. To attenuate the approximation error, a robust adaptive law is employed. The fuzzy compensator and the sliding mode controller work in parallel to achieve the robust formation maneuvers. The SMC law and the robust adaptive law are derived from the Lyapunov's direct method. The feasibility, validity and robustness of the proposed approach are illustrated by a multi-robot system. Compared with the results via the sole SMC method without compensator, the proposed approach can improve the tracking performance. The benefit we can earn from the proposed approach is that the approach is only subject to the mild assumption that the uncertainties have an unknown boundary.

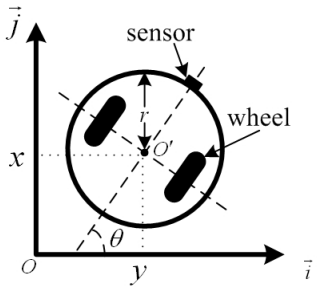

Fig. 1. Schematic of the nonholonomic mobile robot

2 MATHEMATICAL MODEL

2.1 Modeling a single robot

The robot in Fig. 1 is unicycle-like. It is round with $2r$ in diameter and has two parallel driven wheels. The wheels are independently controlled by two DC motors and they are with the same axis. One wheel is mounted on each side of the robot's center. Since the robot is capable of simultaneous arbitrary rotation and translation in the horizontal plane, it can be described by a 3-dimensional vector $\tau = [x\ y\ \theta]^T$. The translational coordinates can be depicted by $(x,\ y)$, which are the midpoint between the two driven wheels. The midpoint is also the center of the round robot. Shown by the dash lines in Fig. 1, another coordinate system fixed on the robot's body is assigned. The rotational coordinate θ, meaning the orientation angle with respect to the fixed frame, can be calculated via the two coordinate systems. To capture the robot's position, a position sensor is located at the front castor.

Consider a multiple robot system composed of N robots. The robots in the group are identical (See in Fig. 1). Assuming that pure rolling and non-slipping motion, the ideal kinematic equations of the nth robot [17] are described by

$$\dot{\tau}_n = \begin{bmatrix} \dot{x}_n \\ \dot{y}_n \\ \dot{\theta}_n \end{bmatrix} = \begin{bmatrix} \cos\theta_n & 0 \\ \sin\theta_n & 0 \\ 0 & 1 \end{bmatrix} \cdot \begin{bmatrix} v_n \\ w_n \end{bmatrix} \qquad (1)$$

where v_n and w_n are the linear and angular velocities of the nth robot, respectively. The assumption means (1) is subject to the following nonholonomic constraint.

$$\begin{bmatrix} -\sin\theta_n & \cos\theta_n & 0 \end{bmatrix} \cdot \dot{\tau}_n = 0 \qquad (2)$$

Consider the variations on the mass and the moment of inertia and the external uncertainties like the slipping

or skidding effects. The dynamic equations to depict the motion of the nth robot [17] are defined by

$$\begin{bmatrix} \ddot{x}_n \\ \ddot{y}_n \\ \ddot{\theta}_n \end{bmatrix} = \begin{bmatrix} -\dot{y}_n\dot{\theta}_n \\ \dot{x}_n\dot{\theta}_n \\ 0 \end{bmatrix} + \begin{bmatrix} \cos\theta_n & 0 \\ \sin\theta_n & 0 \\ 0 & 1 \end{bmatrix} \mathbf{u}_n + \begin{bmatrix} \cos\theta_n & 0 \\ \sin\theta_n & 0 \\ 0 & 1 \end{bmatrix} \Delta_n\mathbf{u}_n + \pi_n(\tau_n, \dot{\tau}_n) \tag{3}$$

here the control input is $\mathbf{u}_n$, defined by $\mathbf{u}_n = [\alpha_n \ \beta_n]^T$. $\alpha = F_n/m_n$ is the robot acceleration and $\beta_n = \sigma_n/J_n$ is the angular acceleration of the robot, where m_n, J_n, F_n and σ_n denote the nominal mass, the nominal moment of inertia, the force and the torque applied to the robot, respectively. Δ_n is the parameter variations, written by

$$\Delta_n = \begin{bmatrix} \varepsilon_n & 0 \\ 0 & \varepsilon_n' \end{bmatrix}$$

here ε_n and ε_n' represent the variations on the mass and the moment of inertia, respectively. In (3), $\pi_n(\tau_n, \dot{\tau}_n)$ written by $[\pi_{nx} \ \pi_{ny} \ \pi_{n\theta}]^T$ means the mixed model uncertainties and external disturbances.

Remark 1: (3) formulates the dynamic model of the single robot with uncertainties in Fig. 1. There are two terms to depict the system uncertainties. Mathematic definitions about the category of uncertainties can be found in [23]. Since Δ_n enters the robot system by the control channel, the parameter variations in (3) belong to matched uncertainties without doubt. Since $\pi_n(\tau_n, \dot{\tau}_n)$ mixes model uncertainties and external disturbances, it is usually mismatched. The two uncertain terms will result in the uncertainties of the following formation dynamics.

2.2 Leader-Follower Formation Scheme

In the group of robots, each robot is with its own kinematic and dynamic models as (1) and (3), respectively. To realize their formation maneuvers, it is necessary to define a control mechanism. The leader-follower approach is such a mechanism to coordinate the robots. The approach is hierarchical. One robot in the group is assigned to be the leader robot. The other robots are named followers. The relationship among the followers is equal to each other. Each follower is cascaded to the leader so that $N-1$ leader-follower pairs exist. Take a leader-follower pair as an example. The follower's motion is decided by the leader. The decision is made in light of the desired distance and the desired relative angle between the follower and the leader.

Without loss of generalization, the ith robot in the group is picked as the leader robot. One robot among all the followers is also selected and index k represents the follower. The pair in Fig. 2 is employed to demonstrate the leader-follower mechanism. Provided that a receiver is located at the centre of the leader robot i, Fig. 2 illustrates the definitions of the distance l_{ik} and the relative angle ψ_{ik} between the leader and the follower. l_{ik} is defined by the distance between the centre of the leader robot i and the front castor of the follower robot k, formulated by

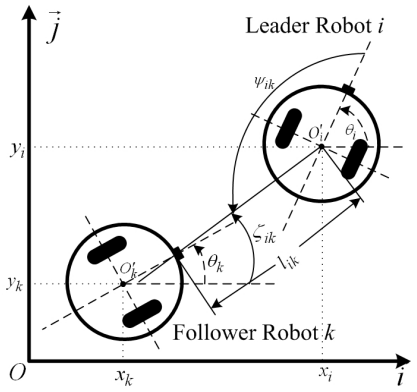

Fig. 2. Schematic of the leader-follower mechanism

$$l_{ik} = \sqrt{(x_i - \bar{x}_k)^2 + (y_i - \bar{y}_k)^2} \tag{4}$$

In (4), the coordinates $(x_i \ y_i)$ denote the centre position of the leader and the coordinates $(\bar{x}_k \ \bar{y}_k)$ denote the caster position of the follower, where $\bar{x}_k = x_k + r\cos\theta_k$, $\bar{y}_k = y_k + r\sin\theta_k$ and r is the radius of the robots.

According to the geometric relationship, ψ_{ik} in Fig. 2 is determined by

$$\psi_{ik} = \pi + \zeta_{ik} - \theta_i \tag{5}$$

here θ_i is the orientation angle of the leader robot i and ζ_{ik} is calculated by

$$\zeta_{ik} = \arctan\frac{y_i - y_k - r\sin\theta_k}{x_i - x_k - r\cos\theta_k} \tag{6}$$

In order to achieve the formation maneuvers, each follower needs to keep at the desired distance and the desired relative angle with respect to the leader. Since the robots are subject to uncertainties, their formation dynamics inherently become uncertain. The motivation of the paper is to develop a control scheme that can form up the robots while resist the adverse effects of uncertainties on the formation stability. To concentrate on the motivation, The following ideal conditions are considered, 1) there are no collisions between the robots, 2) there is no communication delay between the leader and all the followers, 3) each follower robot knows not only its own position and velocity but also the corresponding information of the leader.

Differentiate (4) and (5) twice with respect to time t and substitute (2) into the derivatives. Then, the second derivatives of l_{ik} and ψ_{ik} can be obtained. Define $\mathbf{T}_{ik} = [l_{ik}\ \psi_{ik}]^T$. The dynamic equations depicting the leader-follower formation maneuvers [11] are described by

$$\ddot{\mathbf{T}}_{ik} = \mathbf{G}_{ik}(\mathbf{I}_2 + \Delta_k)\mathbf{u}_k + \mathbf{L}_{ik}(\mathbf{I}_2 + \Delta_i)\mathbf{u}_i + \mathbf{F}_{ik} + \mathbf{P}_{ik} \quad (7)$$

where $\mathbf{I}_2$ is a 2×2 identity matrix, $\mathbf{G}_{ik}$ is written by

$$\mathbf{G}_{ik} = \begin{bmatrix} \cos\phi_{ik} & r\sin\phi_{ik} \\ \frac{-\sin\phi_{ik}}{l_{ik}} & \frac{r\cos\phi_{ik}}{l_{ik}} \end{bmatrix}$$

$\mathbf{L}_{ik}$ is described by

$$\mathbf{L}_{ik} = \begin{bmatrix} -\cos\psi_{ik} & 0 \\ \frac{\sin\psi_{ik}}{l_{ik}} & -1 \end{bmatrix}$$

here $\phi_{ik} = \psi_{ik} + \theta_{ik}$ and $\theta_{ik} = \theta_i - \theta_k$. Further, $\mathbf{F}_{ik} = [F_1\ F_2]^T$ and $\mathbf{P}_{ik} = [P_1\ P_2]^T$ are given as follows.

$$\begin{aligned} F_1 = {} & (\dot{\psi}_{ik})^2 l_{ik} + 2\dot{\psi}_{ik}\dot{\theta}_i l_{ik} + (\dot{\theta}_i)^2 l_{ik} - r\cos\phi_{ik}(\dot{\theta}_k)^2 \\ & -(\dot{y}_k\dot{\theta}_k - \dot{y}_i\dot{\theta}_i)\cos(\psi_{ik}+\theta_i) - (\dot{x}_i\dot{\theta}_i - \dot{x}_k\dot{\theta}_k)\sin(\psi_{ik}+\theta_i) \end{aligned}$$

$$\begin{aligned} F_2 = {} & \frac{-(\dot{y}_k\dot{\phi}_{ik} - \dot{\psi}_{ik}\dot{y}_i)\sin(\psi_{ik}+\theta_i) - (\dot{x}_k\dot{\phi}_{ik} - \dot{\psi}_{ik}\dot{x}_i)\cos(\psi_{ik}+\theta_i) - r\dot{\theta}_k\dot{\phi}_{ik}\sin\phi_{ik}}{l_{ik}} \\ & + \frac{\dot{l}_{ik}((\dot{y}_i - \dot{y}_k)\cos(\psi_{ik}+\theta_i) - (\dot{x}_i - \dot{x}_k)\sin(\psi_{ik}+\theta_i) - r\dot{\theta}_k\cos\phi_{ik})}{{l_{ik}}^2} \end{aligned}$$

$$\begin{aligned} P_1 = {} & -(\pi_{ix} - \pi_{kx})\cos(\psi_{ik}+\theta_i) - (\pi_{iy} - \pi_{ky})\sin(\psi_{ik}+\theta_i) \\ & + r\pi_{k\theta}\sin\phi_{ik} \end{aligned}$$

$$P_2 = \frac{\begin{array}{l}(\pi_{ix} - \pi_{kx})\sin(\psi_{ik}+\theta_i) \\ -(\pi_{iy} - \pi_{ky})\cos(\psi_{ik}+\theta_i) + r\pi_{k\theta}\cos\phi_{ik} - l_{ik}\pi_{i\theta}\end{array}}{l_{ik}}$$

Define $\mathbf{x}_{ik} = [x_{1_{ik}}\ x_{2_{ik}}]^T = [l_{ik}\ \psi_{ik}]^T$. Then, the following state equations are deduced from (7).

$$\ddot{\mathbf{x}}_{ik} = \mathbf{G}_{ik}\mathbf{u}_k + \mathbf{d}_{ik}(\mathbf{x}_{ik}, \dot{\mathbf{x}}_{ik}, t) \quad (8)$$

where $\mathbf{d}_{ik}(\mathbf{x}_{ik}, \dot{\mathbf{x}}_{ik}, t) = \mathbf{G}_{ik}\Delta_k\mathbf{u}_k + \mathbf{L}_{ik}(\mathbf{I}_2 + \Delta_i)\mathbf{u}_i + \mathbf{F}_{ik} + \mathbf{P}_{ik}$.

In the mentioned literature about the SMC-based formation maneuvers [17–20], one common assumption is that the uncertain term $\mathbf{d}_{ik}$ has a known boundary. However, the assumption is too strict to be satisfied in reality. Owing to the invariance of SMC, this paper considers that these uncertainties are mismatched with an unknown boundary. To achieve the formation maneuvers under the challenging assumption, a fuzzy compensator will be designed to attack the issue.

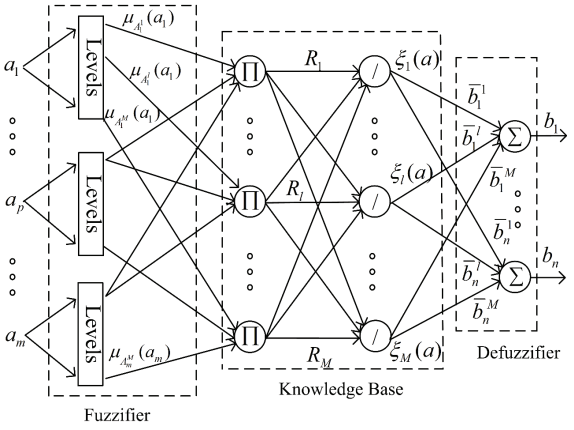

Fig. 3. Prototype of the FIS

Remark 2: $\mathbf{d}_{ik}(\mathbf{x}_{ik}, \dot{\mathbf{x}}_{ik}, t)$ depicts all the uncertainties and it consists of 4 parts. $G_{ik}\Delta_k\mathbf{u}_k$, meaning the parameter variations of the robot k, is matched. Since the leader-follower cooperative mechanism (7) is applied to the follower k, $\mathbf{L}_{ik}(\mathbf{I}_2 + \Delta_i)\mathbf{u}_i$ is hardly matched (The part can hardly enter the control channel of the follower k). Further, $\mathbf{F}_{ik}$ and $\mathbf{P}_{ik}$ are the aggregative representatives of model uncertainties and external disturbances caused by slipping, skidding, friction, drag, etc., which are inherently mismatched.

3 CONTROL DESIGN AND ANALYSIS

3.1 Design of Fuzzy Compensator

A fuzzy inference system (FIS) consists of four parts: knowledge base, fuzzifier, fuzzy inference engine and defuzzifier, where the knowledge base is composed of some fuzzy IF-THEN rules and the fuzzy inference engine employs the rules. This section considers a multi-input multi-output FIS. The structure of this FIS is displayed in Fig. 3, where the input vector is $\mathbf{a} = [a_1,\ a_2,\ \ldots,\ a_m]^T \in \Re^m$, the output vector $\mathbf{b} = [b_1,\ b_2,\ \ldots,\ b_n]^T \in \Re^n$ and every element in $\mathbf{a}$ and $\mathbf{b}$ is scalar. The multi-input multi-output IF-THEN rules can be expressed by

$$R = \cup_{l=1}^{M} R_l \quad (9)$$

In (9), R indicates a collection of fuzzy rules, M denotes the total number of rules and the lth rule is described by

$$\begin{array}{c} R_l : \text{IF } a_1 \text{ is } A_1^l \text{ and } a_2 \text{ is } A_2^l \ \ldots\ a_m \text{ is } A_m^l \\ \text{THEN } b_1 \text{ is } B_1^l \ \ldots \text{ and } b_n \text{ is } B_n^l \end{array} \quad (10)$$

A_p^l and B_q^l in (10) are the linguistic variables of the fuzzy sets, where $p = 1,\ 2,\ \ldots,\ m$ and $q = 1,\ 2, \ldots,\ n$. Both the linguistic variables are determined by their

membership functions $\mu_{A_p^l}(a_p)$ and $\mu_{B_q^l}(b_q)$, here $l = 1, 2, \ldots, M$.

Adopting the singleton fuzzifier mapping, the product inference engine and the center-average defuzzifier mapping, the qth output of the FIS has a form of

$$b_q = \sum_{l=1}^{M} \bar{b}_q^l \xi_l(\mathbf{a}) = \Theta_q^T \xi(\mathbf{a}) \tag{11}$$

In (11), $\xi(\mathbf{a}) = [\xi_1(\mathbf{a}), ..., \xi_M(\mathbf{a})]^T \in \Re^M$ is the fuzzy basis functions vector, where $\xi_l(\mathbf{a})$ is calculated by

$$\xi_l(\mathbf{a}) = \frac{\prod_{p=1}^{m} \mu_{A_p^l}(a_p)}{\sum_{l=1}^{M} (\prod_{p=1}^{m} \mu_{A_p^l}(a_p))}$$

$\Theta_q = [\bar{b}_q^1, ..., \bar{b}_q^M]^T \in \Re^M$ is named the parameter vector, where $\bar{b}_q^l$ is an adaptively adjustable parameter. The vector is the qth column of an $M \times n$ parameter matrix Θ.

Associated with the application of the FIS, the purpose is to approximate the system uncertainties in (8) so that the approximate values are definitely selected as the FIS outputs, i.e., $\mathbf{b} = \hat{\mathbf{d}}_{ik}(\mathbf{x}_{ik},\ \dot{\mathbf{x}}_{ik},\ t)$. Moreover, the system uncertainties in (8) are functions of $\mathbf{x}_{ik}$ and $\dot{\mathbf{x}}_{ik}$ so that l_{ik}, ψ_{ik}, $\dot{l}_{ik}$ and $\dot{\psi}_{ik}$ are picked up as the FIS inputs, i.e., $\mathbf{a} = [l_{ik},\ \psi_{ik},\ \dot{l}_{ik},\ \dot{\psi}_{ik}]^T$.

The linguistic labels of A_p^l are chosen as five levels, i.e., NB, NS, ZO, PS and PB. The labels denote negative big, negative small, zero, positive small and positive big, respectively. The membership function of A_p^l is Gaussian, defined by

$$\mu_{A_p^l}(a_p) = \exp\left(-\frac{(a_p - c_p)^2}{2o_p^2}\right) \tag{12}$$

where c_p and o_p are the center and width of the Gaussian membership function to describe the linguistic variable A_p^l and $p = 1,\ 2,\ 3,\ 4$.

From (11), the approximate values $\hat{\mathbf{d}}_{ik}(\mathbf{x}_{ik}, \dot{\mathbf{x}}_{ik}, t)$ can be calculated by $\hat{\mathbf{d}}_{ik}(\mathbf{x}_{ik}, \dot{\mathbf{x}}_{ik}|\Theta)$, written by

$$\begin{aligned} \hat{\mathbf{d}}_{ik}(\mathbf{x}_{ik}, \dot{\mathbf{x}}_{ik}|\Theta) &= \begin{bmatrix} \hat{d}_{ik,1}(\mathbf{x}_{ik}, \dot{\mathbf{x}}_{ik}|\Theta) \\ \hat{d}_{ik,2}(\mathbf{x}_{ik}, \dot{\mathbf{x}}_{ik}|\Theta) \end{bmatrix} \\ &= \Theta^T \xi(\mathbf{x}_{ik}, \dot{\mathbf{x}}_{ik}) \\ &= \begin{bmatrix} \Theta_1^T \xi(\mathbf{x}_{ik}, \dot{\mathbf{x}}_{ik}) \\ \Theta_2^T \xi(\mathbf{x}_{ik}, \dot{\mathbf{x}}_{ik}) \end{bmatrix} \end{aligned} \tag{13}$$

here $\Theta \in \Re^{625\times 2}$ and $\xi(\mathbf{x}_{ik}, \dot{\mathbf{x}}_{ik}) \in \Re^{625\times 1}$.

Assuming that an optimal parameter matrix Θ^* exists [25], the matrix Θ^* has a form of

$$\Theta^* = \arg\min_{\Theta\in\chi_0}[\sup||\hat{\mathbf{d}}_{ik}(\mathbf{x}_{ik}, \dot{\mathbf{x}}_{ik}|\Theta) - \mathbf{d}_{ik}(\mathbf{x}_{ik}, \dot{\mathbf{x}}_{ik}, t)||] \tag{14}$$

where χ_0 is a proper compact set. Considering the assumption, the minimum approximate errors vector can be determined by

$$\rho = \hat{\mathbf{d}}_{ik}(\mathbf{x}_{ik}, \dot{\mathbf{x}}_{ik}|\Theta^*) - \mathbf{d}_{ik}(\mathbf{x}_{ik}, \dot{\mathbf{x}}_{ik}, t) \tag{15}$$

here $\rho = [\rho_1, \rho_2]^T \in \Re^2$.

The designed FIS is a 4-input- 2-output system and the linguistic variables of the inputs are divided into 5 levels. Consequently, the FIS covers 5^4 fuzzy rules in its knowledge base. There are two ways to reduce the number of fuzzy rules. One is to cut the number of inputs. The other is to reduce the number of levels. From (8), the uncertain term $\mathbf{d}_{ik}(\mathbf{x}_{ik}, \dot{\mathbf{x}}_{ik}, t)$ is functions of $\mathbf{x}_{ik}$ and $\dot{\mathbf{x}}_{ik}$. Once the number of inputs is decreased, the FIS may not work because it cannot obtain enough information. Once the number of levels is reduced, the accuracy of the FIS will definitely decrease. The accuracy of the FIS may increase if the number of levels is increased. But the increase will result in computational burden. Here, the number of levels is selected as 5 by a trade-off between accuracy and computational burden.

Remark 3: It has been proven that fuzzy systems in the form of (11) can approximate continuous function over a compact set to an arbitrary degree of accuracy provided that enough number of rules is given [25]. Here the ability of approximation of the FIS is employed to approximate the unknown uncertainties.

3.2 Design of Sliding Mode Controller

To coordinate the leader-follower pair in Fig. 2 by a sliding mode controller, the sliding surfaces vector is defined by

$$\mathbf{s}_{ik}(t) = \dot{\mathbf{x}}_{ik}^e + \lambda \mathbf{x}_{ik}^e \tag{16}$$

here $\mathbf{s}_{ik}(t) = [s_{ik,1}(t)\ s_{ik,2}(t)]^T \in \Re^2$, $\mathbf{x}_{ik}^e = \mathbf{x}_{ik} - \mathbf{x}_{ik}^d \in \Re^2$ is the state tracking errors vector, $\mathbf{x}_{ik}^d$ is the desired trajectories vector and λ is a 2×2 positive-definite matrix.

Pointed out by V.I. Utkin [23], the SMC method covers two stages. One is sliding mode stage. The other is reaching mode stage. On the reaching mode stage, the system states in (8) tend to the sliding surfaces vector (16) in the state space. On the sliding mode stage, not only the SMC system is of invariance against matched uncertainties, but also the formation dynamics can be described by

$$\mathbf{s}_{ik} = \mathbf{0}_2 \tag{17}$$

Here $\mathbf{0}_2 = [0\ 0] \in \Re^2$. Substituting (16) into (17) yields

$$\dot{\mathbf{x}}_{ik}^e(t) = -\lambda \mathbf{x}_{ik}^e(t) \tag{18}$$

(18) indicates that the formation performance is determined by the eigenvector of the matrix λ on the sliding

mode stage. However, neither (17) nor (18) holds true in the reaching mode stage. For the sake of formula expression, a reference vector is introduced as

$$\delta(t) = \dot{\mathbf{x}}_{ik}^{d}(t) - \lambda \mathbf{x}_{ik}^{e}(t) \tag{19}$$

Finally, the SMC-based control law is designed as

$$\mathbf{u}_k = -\mathbf{G}_{ik}^{-1}[\hat{\mathbf{d}}_{ik}(\mathbf{x}_{ik}, \dot{\mathbf{x}}_{ik}|\Theta) - \dot{\delta} + \kappa \mathbf{s}_{ik} + \eta \mathrm{sign}(\mathbf{s}_{ik})] \tag{20}$$

where $\kappa = \mathrm{diag}\{\kappa_1,\ \kappa_2\}$, $\eta = \mathrm{diag}\{\eta_1,\ \eta_2\}$, κ_1, κ_2, η_1, and η_2 are predefined parameters. Further, $\mathrm{sign}(\mathbf{s}_{ik})$ is defined by $\mathrm{sign}(\mathbf{s}_{ik}) = [\mathrm{sign}(s_{ik,1}(t)),\ \mathrm{sign}(s_{ik,2}(t))]^T$.

In (20), the control signal $\mathbf{u}_i$ of the leader i actually exists as disturbances for the follower k. Since the task of the leader i is to track a predefined trajectory, the leader's control problem can be considered as the trajectory tracking of a single robot. There has been a great deal of work in this field and different control methods have been developed. Usually, it is directly assumed that the leader robot is well controlled by a developed technology [9].

3.3 Stability Analysis

Theorem 1: Define the sliding surfaces vector (16), design the fuzzy compensator (13) and adopt the control law (20). The SMC-based formation control system with fuzzy compensator is of asymptotical stability if

$$\dot{\Theta}_q = {\Gamma_q}^{-1} s_{ik,q} \xi(\mathbf{x}_{ik}, \dot{\mathbf{x}}_{ik}) \tag{21}$$

where $\Gamma_q > 0 \in \Re^1$, $\kappa_q > 0$, $\eta_q > |\rho_q|$ and $q = 1,\ 2$.

Proof: Take the following positive definite function into account as a Lyapunov candidate function.

$$V(t) = \frac{1}{2}(\mathbf{s}_{ik}^T \mathbf{s}_{ik} + \sum_{q=1}^{2} \tilde{\Theta}_q^T \Gamma_q \tilde{\Theta}_q) \tag{22}$$

where $\tilde{\Theta}_q = \Theta_q^* - \Theta_q$ and Θ_q^* is the qth column vector of the optimal parameter matrix Θ^*.

Differentiating (22) with respect to time t gives

$$\dot{V}(t) = \mathbf{s}_{ik}^T \cdot \dot{\mathbf{s}}_{ik} + \sum_{q=1}^{2} \tilde{\Theta}_q^T \Gamma_q \dot{\tilde{\Theta}}_q \tag{23}$$

From (16) and (19), (24) can be obtained.

$$\mathbf{s}_{ik}(t) = \dot{\mathbf{x}}_{ik}(t) - \delta(t) \tag{24}$$

Differentiating (24) with respect to time t and substituting the first derivative of $\mathbf{s}_{ik}$ into (23) yields

$$\dot{V}(t) = \mathbf{s}_{ik}^T \cdot (\ddot{\mathbf{x}}_{ik} - \dot{\delta}) + \sum_{q=1}^{2} \tilde{\Theta}_q^T \Gamma_q \dot{\tilde{\Theta}}_q \tag{25}$$

From (8), (26) can be formulated by

$$\dot{V}(t) = \mathbf{s}_{ik}^T \cdot [\mathbf{G}_{ik}\mathbf{u}_k + \mathbf{d}_{ik}(\mathbf{x}_{ik}, \dot{\mathbf{x}}_{ik}, t) - \dot{\delta}] + \sum_{q=1}^{2} \tilde{\Theta}_q^T \Gamma_q \dot{\tilde{\Theta}}_q \tag{26}$$

Substitute (15) and (20) into (26). Then, (27) can be drawn

$$\begin{aligned}
\dot{V}(t) = & -\mathbf{s}_{ik}^T \cdot [\hat{\mathbf{d}}_{ik}(\mathbf{x}_{ik}, \dot{\mathbf{x}}_{ik}|\Theta) - \mathbf{d}_{ik}(\mathbf{x}_{ik}, \dot{\mathbf{x}}_{ik}, t) + \kappa \mathbf{s}_{ik} \\
& + \eta \mathrm{sign}(\mathbf{s}_{ik})] + \sum_{q=1}^{2} \tilde{\Theta}_q^T \Gamma_q \dot{\tilde{\Theta}}_q \\
= & -\mathbf{s}_{ik}^T [\hat{\mathbf{d}}_{ik}(\mathbf{x}_{ik}, \dot{\mathbf{x}}_{ik}|\Theta) + \rho - \hat{\mathbf{d}}_{ik}(\mathbf{x}_{ik}, \dot{\mathbf{x}}_{ik}|\Theta^*) + \kappa \mathbf{s}_{ik} \\
& + \eta \mathrm{sign}(\mathbf{s}_{ik})] + \sum_{q=1}^{2} \tilde{\Theta}_q^T \Gamma_q \dot{\tilde{\Theta}}_q \\
= & -\mathbf{s}_{ik}^T [\rho + \kappa \mathbf{s}_{ik} + \eta \mathrm{sign}(\mathbf{s}_{ik}) - \tilde{\Theta}^T \xi(\mathbf{x}_{ik}, \dot{\mathbf{x}}_{ik})] \\
& + \sum_{q=1}^{2} \tilde{\Theta}_q^T \Gamma_q \dot{\tilde{\Theta}}_q \\
= & -\mathbf{s}_{ik}^T \rho - \mathbf{s}_{ik}^T \kappa \mathbf{s}_{ik} - \mathbf{s}_{ik}^T \eta \mathrm{sign}(\mathbf{s}_{ik}) \\
& + \sum_{q=1}^{2} [\tilde{\Theta}_q^T \Gamma_q \dot{\tilde{\Theta}}_q + \mathbf{s}_{ik,q} \tilde{\Theta}_q^T \xi(\mathbf{x}_{ik}, \dot{\mathbf{x}}_{ik})]
\end{aligned} \tag{27}$$

Adopting the robust adaptive law (21), (27) becomes

$$\dot{V}(t) = -\mathbf{s}_{ik}^T \rho - \mathbf{s}_{ik}^T \kappa \mathbf{s}_{ik} - \mathbf{s}_{ik}^T \eta \mathrm{sign}(\mathbf{s}_{ik}) \tag{28}$$

Substituting $\eta_q > |\rho_q|$ into (28) yields

$$\dot{V}(t) \leqslant -\mathbf{s}_{ik}^T \kappa \mathbf{s}_{ik} < 0 \tag{29}$$

(29) means that the Lyapunov function (22) satisfies $\dot{V}(t) < 0$. Consequently, the SMC-based formation control system with fuzzy compensator is asymptotically stable in the sense of Lyapunov once the robust adaptive law (21) is adopted. □

$\mathbf{d}_{ik}(\mathbf{x}_{ik}, \dot{\mathbf{x}}_{ik}, t)$ is mismatched and it has an unknown boundary. Owing to its adverse effects, the stability of the formation system cannot be guaranteed by the invariance of SMC. In order to guarantee the system stability, the designed FIS is employed to approximate $\mathbf{d}_{ik}(\mathbf{x}_{ik}, \dot{\mathbf{x}}_{ik}, t)$ so that the SMC-based formation controller has the ability against the adverse effects of mismatched uncertainties.

Remark 4: $\mathbf{G}_{ik}$ is invertible. $\mathbf{G}_{ik}$ is formulated by (7). $\det(\mathbf{G}_{ik}) = \frac{r}{l_{ik}} < 1$. Note that l_{ik} is formulated by the distance between the center of the leader i and the front castor of the follower k, that is, l_{ik} is always larger than r.

4 SIMULATION RESULTS

The designed robust adaptive control scheme is composed of one sliding mode controller and one fuzzy compensator. The structure of the presented control scheme is illustrated in Fig. 4. Concerning the control structure,

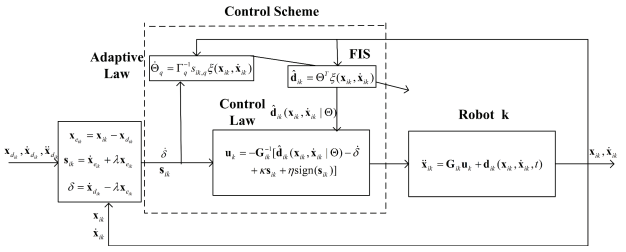

Fig. 4. Structure of the control scheme

the fuzzy compensator is located at the feedforward channel and cooperates with the sliding mode controller placed at the feedback channel. The compensator and controller work in parallel to achieve the formation maneuvers. To demonstrate the feasibility, validity and robustness of such a control scheme, some simulations are performed via a multi-robot system and the results are discussed in this section.

The multi-robot system consists of one leader and two followers. The three mobile robots are identical (See in Fig. 1). Each robot is 0.05m in radius. The leader is controlled by the kinematic based sliding mode controller to track its predefined trajectories [30]. The two followers each have the presented robust adaptive control scheme (20) to track their leader, independently. The formation objective is to make the two followers maintain their desired distances and relative angles with respect to the leader in the presence of uncertainties.

The parameter variations matrixes of the three robots are considered by

$$\Delta_i = \Delta_k = \begin{bmatrix} 0.3\times \mathrm{rand}() - 0.15 & 0 \\ 0 & 0.3\times \mathrm{rand}() - 0.15 \end{bmatrix} \tag{30}$$

here $i = 1$ denotes the leader and $k = 2,\ 3$ denotes the two followers. rand() is a MATLAB command and it generates a uniformly distributed random number on the open interval $(0,\ 1)$.

From (3), Δ_n indicates the parameter variations such that (30) means that the payload variations on the mass and the moment of inertia are as much as maximum $\pm 15\%$ of the nominal parameters. The reason that we consider the 15% variation is that each robot is driven by two DC motors. The 15% parameter variation is enough to cover the regular parameter perturbation. Excessive variation may result in motor overload in practice.

Furthermore, P_{ik} in (8) is related to π_n in (3). Note that $\pi_{ix} - \pi_{kx}$ and $\pi_{iy} - \pi_{ky}$ exist in P_{ik}, meaning that it is not representative to define $\pi_i = \pi_k$. Here, the following different functions are assigned to the leader and the two followers, defined by

$$\begin{aligned} \pi_{ix} = \pi_{iy} = \pi_{i\theta} &= 0.5\sin(2\pi t) \\ \pi_{kx} = \pi_{ky} = \pi_{k\theta} &= 0.2\sin(\pi t) \end{aligned} \tag{31}$$

All the widths in (12) are set by $\frac{\sqrt{2}\pi}{8}$. Since the linguistic variables are divided into 5 levels, the centers of c_p are set by $-\frac{\pi}{2}$, $-\frac{\pi}{4}$, 0, $\frac{\pi}{4}$, $\frac{\pi}{2}$, respectively. Other parameters in (21) are selected by $\Gamma_1 = \Gamma_2 = 0.00005$. Additionally, the parameter matrix λ in (16) is chosen as $\lambda = \begin{bmatrix} 2.3 & 0 \\ 0 & 2 \end{bmatrix}$. κ and η in (20) are determined by $\kappa = \begin{bmatrix} 5 & 0 \\ 0 & 15 \end{bmatrix}$ and $\eta = \begin{bmatrix} 0.5 & 0 \\ 0 & 0.5 \end{bmatrix}$, respectively.

4.1 Line Formation Moving in Circular Trajectories

Consider a set of concentrically circular trajectories. The initial posture vector of the leader is located at $\tau_1 = [0.5\mathrm{m}\ \ 0\mathrm{m}\ \ \frac{1}{2}\pi\mathrm{rad}]^T$. The initial posture vectors of the two followers are set by $\tau_2 = [0.8\mathrm{m}\ \ -0.4\mathrm{m}\ \ 0\mathrm{rad}]^T$ and $\tau_3 = [1\mathrm{m}\ \ 0.5\mathrm{m}\ \ \pi\mathrm{rad}]^T$, respectively.

According to the above initial posture vectors, the initial distances and relative angles of the two followers with respect to the leader can be calculated as $\mathbf{x}_{12}^0 = [0.5\mathrm{m}\ \ \frac{3.2}{4}\pi\mathrm{rad}]^T$ and $\mathbf{x}_{13}^0 = [0.707\mathrm{m}\ \ \frac{3}{4}\pi\mathrm{rad}]^T$. The desired system states of the two followers are set by $\mathbf{x}_{12}^d = [0.13\mathrm{m}\ \ \frac{1}{2}\pi\mathrm{rad}]^T$ and $\mathbf{x}_{13}^d = [0.26\mathrm{m}\ \ \frac{1}{2}\pi\mathrm{rad}]^T$. The desired linear and angular velocities of the leader robot are set by $v_1^d = 0.5\mathrm{m/s}$ and $w_1^d = 1\mathrm{rad/s}$.

Fig. 5 demonstrates the group of robots forms up a line formation while moving in the concentrically circular trajectories, where the colorful squares denote the initial positions of the three robots and the colorful circles indicate the robots in the dynamic process. In each square or circle, the arrow means the orientation angle of the robot. To demonstrate their postures and formation, the black dash in Fig. 5 bonds the robots together at the same moment. From Fig. 5, the two followers follow the leader and keep the desired distances and the desired relative angles.

To demonstrate the formation performance of the presented control scheme, the comparisons between the designed robust adaptive SMC method (R-A SMC) and the sole SMC method are shown in Figs. 6-9, where the parameters of the sole sliding mode controller are kept uncharged from the presented control scheme.

The curves in Fig. 6a and b illustrate the distance l_{12} and the relative angle ψ_{12} between Leader 1 and Follower 2, respectively. In Fig. 6c and d, the distance l_{13} and the relative angle ψ_{13} between Leader 1 and Follower 3 are displayed. Fig. 7a and b shows the control inputs α_2 and β_2 of Follower 2. The curves of the control inputs α_3 and

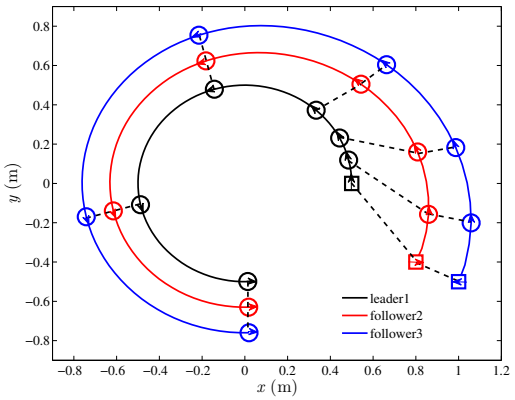

Fig. 5. Straight line formation of the multi-robot system while moving in concentric circles

β_3 of Follower 3 are demonstrated in Fig. 7c and d. The sliding-surface vectors of the two followers are shown in Fig. 8. Fig. 9 illustrates the outputs of the designed FIS.

From Fig. 6, the performance of the presented control scheme is better without doubt. In Fig. 6, the curves by the sole sliding mode controller apparently fluctuate in the dynamic process because the controller cannot adaptively resist unknown uncertainties. This fact indicates the two followers sway to and fro in practice. As a result, the formation maneuver by the sole SMC method is not as accurate as expected. In contrast, the curves by the presented control scheme are much smoother.

In Fig. 7, the curves by both the methods dramatically jump back and forth. The phenomenon is chattering, a drawback of the SMC methodology. The jumping points in Fig. 7 are different in each of the simulations because the uncertainties in (31) are random. To overcome the phenomenon, one can employ a saturation function instead of the signum function in (20).

Proven in Theorem 1, the sliding-surface vectors in Fig. 8 are of asymptotic stability in the presence of mismatched uncertainties. The SMC-based controller and the fuzzy compensator work together to realize the robust formation control of the group of uncertain robots.

The uncertainties term $\mathbf{d}_{ik}$ and its approximations by the fuzzy compensator are illustrated in Fig. 9. From Fig. 9, the outputs of the designed FIS have apparent errors at the outset because the FIS is updating the system parameter matrix Θ in terms of the robust adaptive law (21) in order to track the unknown uncertainties. Finally, the FIS outputs can track the uncertainties and the formation performance can be improved by the fuzzy compensator.

4.2 More Formation Maneuvers

Fig. 10 demonstrates the group of robots forms up a triangle when moving along the concentric circles. In Fig. 10, the initial posture vectors of the three robots are kept unchanged from the numerical example in Subsection 4.1. Accordingly, the initial distances and relative angles of the two followers with respect to the leader are also kept unchanged. The desired system states of the two followers are set by $\mathbf{x}_{12}^d = [0.13\text{m} \;\; \frac{1}{4}\pi\text{rad}]^T$ and $\mathbf{x}_{13}^d = [0.26\text{m} \;\; \frac{1}{2}\pi\text{rad}]^T$. The controller and compensator parameters are also kept unchanged from the aforementioned straight line formation in the concentric circlers.

Fig. 11 illustrates the multi-robot system forms up a straight line when moving along sinusoidal trajectories. In Fig. 11, the initial posture vector of the leader is set by $\tau_1 = [0\text{m} \; 0\text{m} \; 0\text{rad}]^{\mathrm{T}}$ and the initial posture vectors of the two followers are set by $\tau_2 = [1\text{m} \;\; -1\text{m} \;\; \frac{3}{4}\pi\text{rad}]$, and $\tau_3 = [-1\text{m} \;\; 1\text{m} \;\; \frac{1}{4}\pi\text{rad}]^{\mathrm{T}}$, respectively. According to the above three initial posture vectors, the initial distances and relative angles of the two followers with respect to the leader are calculated as $\mathbf{x}_{12}^0 = [\sqrt{2}\text{m} \;\; \frac{3}{4}\pi]^{\mathrm{T}}$ and $\mathbf{x}_{13}^0 = [\sqrt{2}\text{m} \;\; -\frac{1}{4}\pi]^{\mathrm{T}}$. The desired system states of the two followers are set by $\mathbf{x}_{12}^d = [0.4\text{m} \;\; \frac{1}{2}\pi]^{\mathrm{T}}$ and $\mathbf{x}_{13}^d = [0.4\text{m} \;\; -\frac{1}{2}\pi\text{rad}]^{\mathrm{T}}$. The desired linear and angular velocities of the leader robot in Fig. 11 are set by $v_1^d = 1\text{m/s}$ and $w_1^d = \sin(t)\text{rad/s}$. The controller and compensator parameters are still kept unchanged. They are the same as the parameters of the aforementioned two formations.

4.3 Extensions

To demonstrate the scalability of the presented control scheme, two more robots are complemented to the aforementioned three-robot simulation platform. The five robots are identical. The presented control scheme is carried out by such an augmented multi-robot system. Displayed in Fig. 12, the five uncertain robots form up a pentagon when moving along straight line trajectories. In Fig. 12, the initial posture vector of the leader is set by $\tau_1 = [0\text{m} \; 0\text{m} \; 0\text{rad}]^T$. The initial posture vectors of the followers are set by $\tau_2 = [0\text{m} \; 0.3\text{m} \; 0\text{rad}]^T$, $\tau_3 = [0\text{m} \; 0.6\text{m} \; 0\text{rad}]^T$, $\tau_4 = [0\text{m} \; -0.3\text{m} \; 0\text{rad}]^T$ and $\tau_5 = [0\text{m} \; -0.6\text{m} \; 0\text{rad}]^T$, respectively. According to these initial posture vectors, the initial distances and relative angles of the four followers with respect to the leader can be calculated as $\mathbf{x}_{12}^0 = [0.3\text{m} \; \frac{\pi}{2}\text{rad}]^T$, $\mathbf{x}_{13}^0 = [0.6\text{m} \; \frac{\pi}{2}\text{rad}]^T$, $\mathbf{x}_{14}^0 = [0.3\text{m} \; -\frac{\pi}{2}\text{rad}]^T$ and $\mathbf{x}_{15}^0 = [0.6\text{m} \; -\frac{\pi}{2}\text{rad}]^T$. To form up and maintain the pentagonal formation, the desired system states of the followers are set by $\mathbf{x}_{12}^d = [0.2\text{m} \; \frac{4}{5}\pi\text{rad}]^T$, $\mathbf{x}_{13}^d = [0.32\text{m} \; \pi\text{rad}]^T$, $\mathbf{x}_{14}^d = [0.32\text{m} \; -\frac{4}{5}\pi\text{rad}]^T$ and $\mathbf{x}_{15}^d = [0.2\text{m} \; -\frac{3}{5}\pi\text{rad}]^T$, respectively. The desired linear and angular velocities of the leader robot are set by $v_1^d = 0.5\text{m/s}$ and $w_1^d = 0\text{rad/s}$. The parameters of the controller and compensator for the

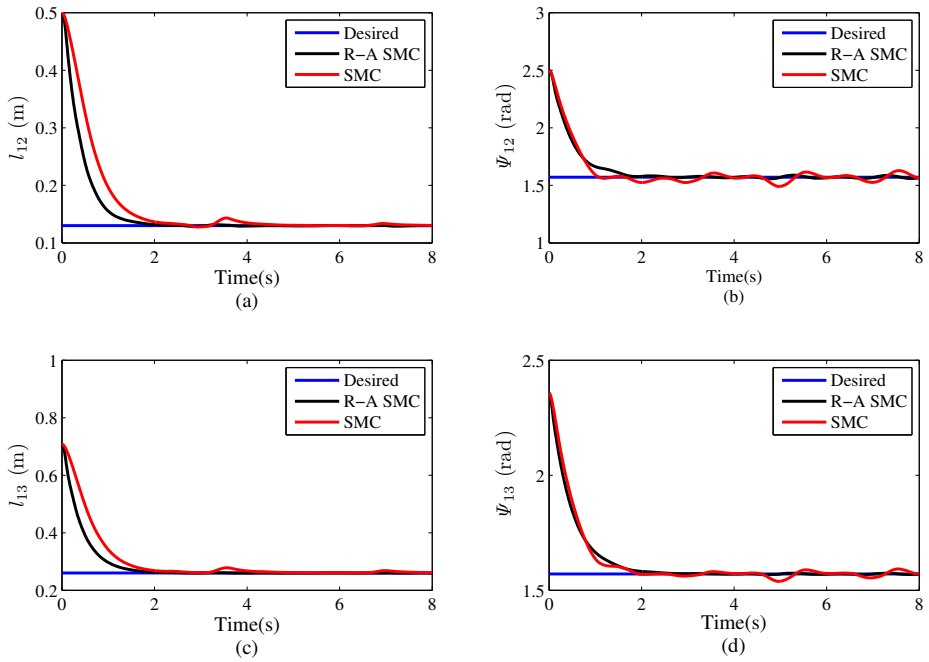

Fig. 6. Distances and relative angles of the two followers with respect to the leader. a. Distance l_{12}, b. Relative angle ψ_{12}, c. Distance l_{13}, d. Relative angle ψ_{13}.

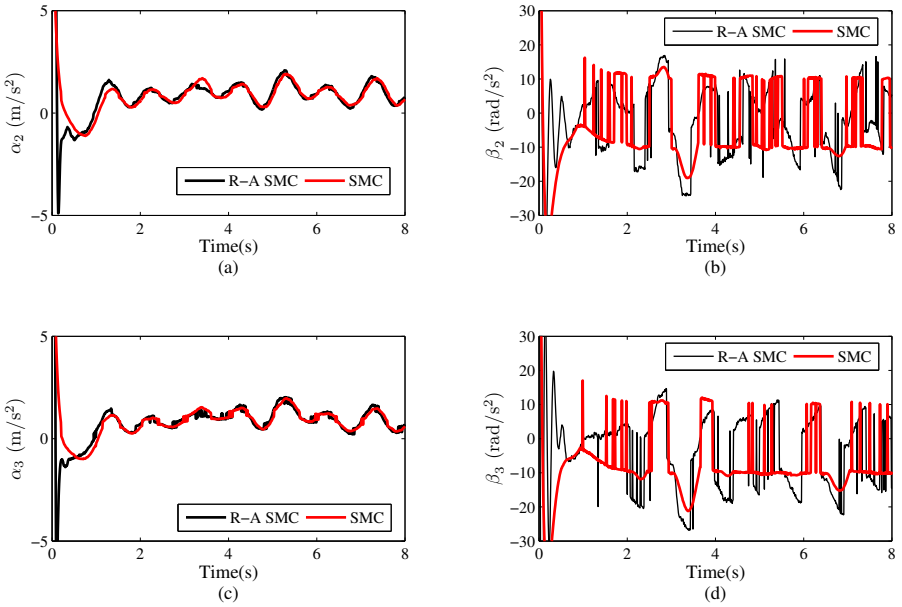

Fig. 7. Accelerations and angular accelerations of the two follower robots. a. Acceleration of Follower 2 α_2, b. Angular acceleration of Follower 2 β_2, c. Acceleration of Follower 3 α_3, d. Angular acceleration of Follower 3 β_3.

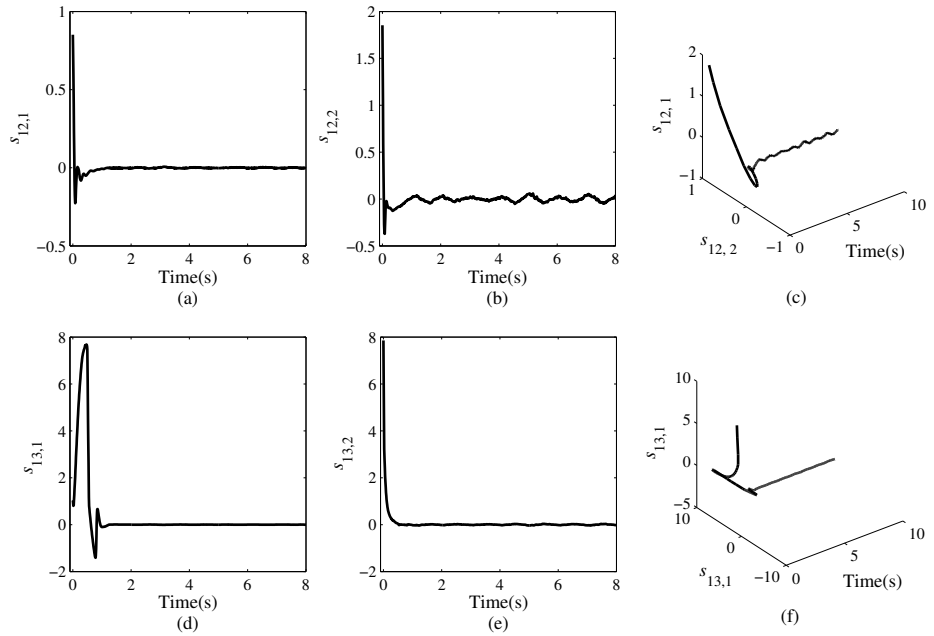

Fig. 8. Sliding-surface vectors and their elements. a. $s_{12,1}$*, b.* $s_{12,2}$*, c three-dimensional plot of the sliding-surface vector* $\mathbf{s}_{12}$*, d.* $s_{13,1}$*, e.* $s_{13,2}$ *and f. three-dimensional plot of the sliding-surface vector* $\mathbf{s}_{13}$*.*

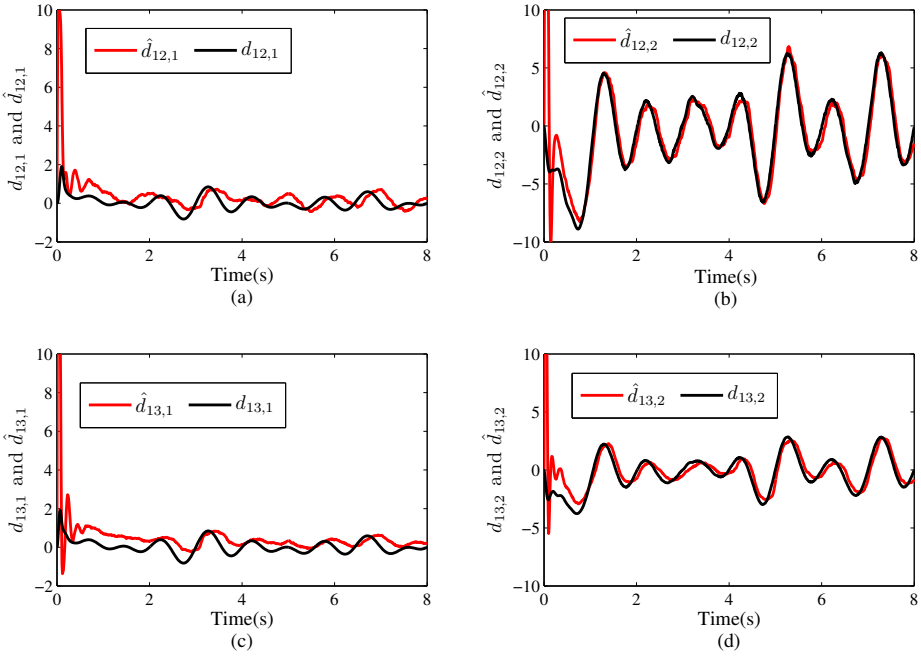

Fig. 9. Uncertain term $\mathbf{d}_{ik}$ *and its approximation* $\hat{\mathbf{d}}_{ik}$*. a.* $d_{12,1}$ *and* $\hat{d}_{12,1}$*, b.* $d_{12,2}$ *and* $\hat{d}_{12,2}$*, c.*$d_{13,1}$ *and* $\hat{d}_{13,1}$*, d.*$d_{13,2}$ *and* $\hat{d}_{13,2}$*.*

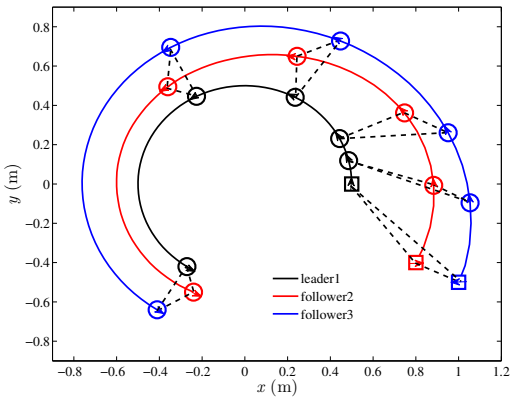

Fig. 10. Triangular formation of the multi-robot system while moving in the concentric circles

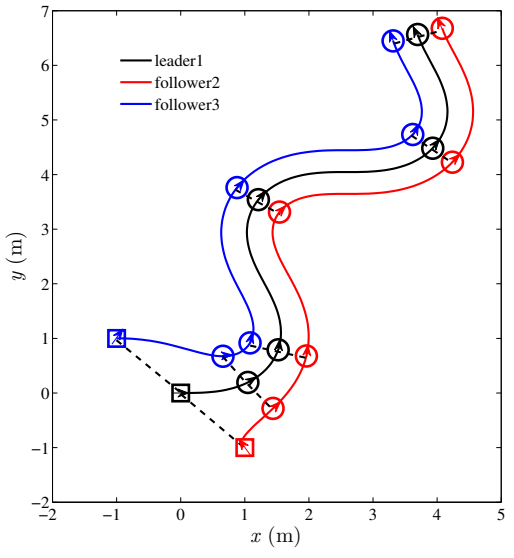

Fig. 11. Straight line formation of the multi-robot system while moving in sinusoidal trajectories

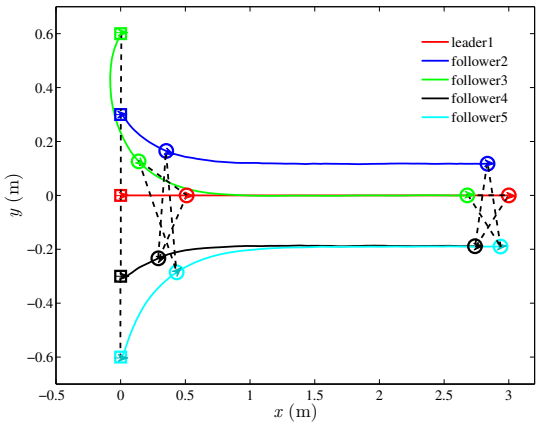

Fig. 12. Pentagon formation of 5 robots while moving in straight lines.

pentagonal formation are still kept unchanged. Although Fig. 12 shows the presented method is scalable, the result is under the assumption that there are no communication problems between the leader and its followers. The assumption is mild enough for small-scale formations but it is rather idealized for large-scale formations.

5 CONCLUSIONS

This paper has addressed the formation control problem for swarms of uncertain mobile robots. The formation mechanism is based on the leader-follower scheme. To suppress the mismatched uncertainties when forming up the robots, the SMC-based control method with fuzzy compensator is employed, where the SMC controller and the fuzzy compensator are located at the feedback and feedforward channels, respectively. The theoretical analysis proves that the coordinated formation control system with mismatched uncertainties is of asymptotic stability in the sense of Lyapunov. The presented control scheme has achieved the formation maneuvers of a multi-robot system composed of three mobile robots. The simulation results have demonstrated the effectiveness, feasibility and scalability of the presented control scheme.

ACKNOWLEDGMENT

This work was partly supported the NSFC Project under Grant No.60904008 and the International Science and Technology Cooperation Project between China and Denmark under Grant No.2014DFG62530.

REFERENCES

[1] M. Al Khawaldah, A. Nuechter, "Multi-robot cooperation for efficient exploration," *Automatika*, vol. 55, no. 3, pp. 276–286, 2014.

[2] K. Kanjanawanishkul, "Coordinated path following for mobile robots using a virtual structure strategy with model predictive control," *Automatika*, vol. 55, no. 3, pp.287–298, 2014.

[3] L. Cheng, Y.P. Wang, W Ren, Z.-G. Hou, M. Tan, "On convergence rate of leader-following consensus of linear multi-agent systems with communication noises," *IEEE Trans. Autom. Control*, vol. 61, no. 11, pp. 3586–3592, 2016.

[4] Y.Dai, Y. Kim, S. Wee, D. Lee, S. Lee, "A switching formation strategy for obstacle avoidance of a multi-robot system based on robot priority model," *ISA Trans.*, vol. 56, pp. 123–134, 2015.

[5] J. Ghommam, H. Mehrjerdi, M. Saad, "Robust formation control without velocity measurement of the leader robot," *Control Eng. Practice*, vol. 21, no. 8, pp. 1143–1156, 2013.

[6] L. Cheng, Z.G. Hou, M. Tan, "A mean square consensus protocol for linear multi-agent systems with communication noises and fixed topologies," *IEEE Trans. Autom. Control*, vol. 59, no. 1, pp. 261–267, 2014.

[7] L. Cheng, Y.P. Wang, Z.G. Hou, M. Tan, Z.Q. Cao, "Sampled-data based average consensus of second-order integral multi-agent systems: switching topologies and communication noises," *Automatica*, vol. 49, no. 5, pp. 1458–1464, 2013.

[8] Y. Cai, Z. Tang, Y. Ding, B. Qian. "Theory and application of multi-robot service-oriented architecture,". *IEEE/CAA J Autom Sinica*, vol. 3, no. 1, pp. 15-25, 2016.

[9] M. Biglarbegian, "A novel robust leader-following control design for mobile robots," *J. Intell. Robot. Syst.*, vol. 71, no. 3-4, pp. 391–402, 2013.

[10] A. Guillet, R. Lenain, B. Thuilot, P. Martinet, "Adaptable robot formation control: adaptive and predictive formation control of autonomous vehicles," *IEEE Robot. Autom. Mag.*, vol. 21, no. 1, pp.28–39, 2014.

[11] D.W. Qian, S.W. Tong, J.R. Guo, S.G. Lee, "Leader-follower-based formation control of nonholonomic mobile robots with mismatched uncertainties via integral sliding mode," *Proc. Inst. Mech. Eng. Part I-J Syst Control Eng.*, vol. 229, no. 6, pp. 559–569, 2015.

[12] W.H. Zhao, T.H. Go, "Quadcopter formation flight control combining MPC and robust feedback linearization," *J. Frankl. Inst.-Eng. Appl. Math.*, vol. 351, no. 3, pp. 1335–1355, 2014.

[13] W. Dong, "Flocking of multiple mobile robots Based on backstepping," *IEEE Trans. Syst. Man Cybern. Part B-Cybern.*, vol. 41, no. 2, pp. 414–424, 2011.

[14] K. Yoshida, H. Fukushima, K. Kon, F. Matsuno, "Control of a group of mobile robots based on formation abstraction and decentralized locational optimization," *IEEE Trans. Robot.*, vol. 30, no. 3, pp. 550–565, 2014.

[15] T. Dierks, S. Jagannathan, "Neural network output feedback control of robot formations," *IEEE Trans. Syst. Man Cybern. Part B-Cybern.*, vol. 40, no. 2, pp. 383–399, 2010.

[16] H.R. Dong, Y.L. Kang, X.X. Yang, X.B. Sun, "Fuzzy control of a class of autonomous formation constrained systems," *Neural Comput. Appl.*, vol. 23, no. 7-8, pp. 1915–1922, 2013.

[17] M. Defoort, T. Floquet, A. Kokosy, W. Perruquetti, "Sliding-mode formation control for cooperative autonomous mobile robots," *IEEE Trans. Ind. Electron.*, vol. 55, no. 11, pp. 3944–3953, 2008.

[18] Y.H. Chang, C.W. Chang, C.L. Chen, C.W. Tao, "Fuzzy sliding mode formation control for multirobot systems: design and implementation," *IEEE Trans. Syst. Man Cybern. Part B-Cybern.*, vol. 42, no. 2, pp. 444–457, 2012.

[19] D.Y. Zhao, T. Zou, "A finite-time approach to formation control of multiple mobile robots with terminal sliding mode," *Int. J. Syst. Sci.*, vol. 43, no. 11, pp. 1998–2014, 2012.

[20] B.S. Park, J.B. Park, Y.H. Choi, "Robust formation control of electrically driven nonholonomic mobile robots via sliding mode technique," *Int. J. Control Autom. Syst.*, vol. 9, no. 5, pp.888–894, 2011.

[21] D.W. Qian, X.J. Liu, J.Q. Yi, "Robust sliding mode control for a class of underactuated systems with mismatched uncertainties," *Proc. Inst. Mech. Eng. Part I-J Syst Control Eng.*, vol. 223, no. 6, pp. 785–795, 2009.

[22] L. Chen, Y. Yan, C. Mu, C. Sun, "Characteristic model-based discrete-time sliding mode control for spacecraft with variable tilt of flexible structures," *IEEE/CAA J Autom Sinica*, vol. 3, no. 1, pp. 42–50, 2016.

[23] V.I. Utkin, *Sliding modes in control and optimization*. 2nd ed. Berlin: Springer-Verlag, 1992.

[24] D.W. Wang, C.B. Low, "Modeling and analysis of skidding and slipping in wheeled mobile robots: control design perspective." *IEEE Trans. Robot.*, vol. 24, no. 3, pp. 676–687, 2008.

[25] L. Wang, *Adaptive Fuzzy Systems and Control-design and Stability Analysis*. Englewood Cliffs, NJ: Prentice-Hall, 1994.

[26] L. Cheng, Z.G. Hou, M. Tan, W.J. Zhang, "Tracking control of a closed-chain five-bar robot with two degrees offreedom by integration of approximation-based approach and mechanical design," *IEEE Trans. Syst. Man Cybern. Part B-Cybern.*, vol. 42, no. 5, pp. 1470–1479, 2012.

[27] J.T. Fei, J. Zhou, "Robust Adaptive Control of MEMS triaxial gyroscope using fuzzy compensator," *IEEE Trans. Syst. Man Cybern. Part B-Cybern.*, vol. 42, no. 6, pp. 1599–1607, 2012.

[28] H.P. Singh, "Simulation of neural network based adaptive compensator control scheme for multiple mobile manipulators with uncertainties," *Int. J. Nonlinear Sci. Numer. Simul.*, vol. 15, no. 3-4, pp. 181–188, 2014.

[29] A. Chatterjee, G. Sarkar, A. Rakshit, "A reinforcement-learning-based fuzzy compensator for a microcontroller-based frequency synthesizer/vector voltmeter," *IEEE Trans. Instrum. Meas.*, vol. 60, no. 9, pp. 3120–3127, 2011.

[30] Y. Kanayama, Y. Kimura, F. Miyazaki, T. Noguchi, "A stable tracking control method for an autonomous mobile robot," in *Proceedings of 1990 IEEE international conference on robotics and automation*, Cincinnati, OH, 13-18 May 1990, 384-389. New York: IEEE.

D. Qian received the B.E. degree from the Hohai University, Nanjing, China, in 2003. He received the M.E. degree from Northeastern University, Shenyang, China, and the Ph.D. degree from the Institute of Automation, Chinese Academy of Sciences, Beijing, China, in 2005 and 2008, respectively. Currently, he is an Associate Professor with the School of Control and Computer Engineering, North China Electric Power University, Beijing, China. His research interests are in the theory and applications of intelligent and nonlinear control.

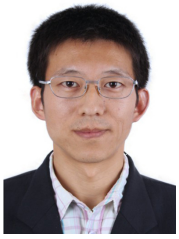

S. Tong received the B.E. degree in chemical engineering from the University of Petroleum (East China), Shandong, China, in 1999, the M.E. degree in control theory and control engineering from the University of Petroleum (Beijing), Beijng, in 2003, and the Ph.D. degree from the Institute of Automation, Chinese Academy of Sciences, Beijing, in 2008. He is currently on staff with the College of Automation at Beijing Union University. His research interests include intelligent control, networked control, proton exchange membrane fuel cells, and their industrial applications.

C. Xu received the bachelor's and master's degrees majored in Thermal Power Engineering from the Northeastern University of China, in 1997 and 2000 respectively, and the Ph.D. degree majored in Power Engineering from the Southeast University of China, in 2005. Currently, he is a professor at Renewable Energy department of Hohai University in China. Dr. Xu's research interests include control applications, solar thermal power system, wind turbine control, wind farm plan and design. He has published over 100 papers in those areas and a book named wind farm plan and design.

AUTHORS' ADDRESSES

Dianwei Qian
North China Electric Power University,
School of Control and Computer Engineering,
No. 2 Beinong Road, Changping District, Beijing, P.R. China
e-mail: dianwei.qian@ncepu.edu.cn

Shiwen Tong
Beijing Union University,
College of Automation,
No. 97 Beisihuan Donglu, Chaoyang District, Beijing 100101, P.R. China
e-mail: shiwen.tong@buu.edu.cn

Chang Xu
Hohai University,
College of Energy and Electricity,
No. 1 Xikang Road, Gulou District, Nanjing 210098, China
e-mail: zhuifengxu@hhu.edu.cn

Received: 2016-01-06
Accepted: 2017-03-27